Enhancing Non-Destructive Testing through Resonant Defect Amplification in Ultrasound-Activated Methods

Astrid E. Werner, Lars R. Jensen

Department of Materials Science and Engineering, University of Michigan, Ann Arbor, MI, USA

Abstract. The presence of a defect leads to a local decrease in rigidity for a certain mass of the material and therefore manifests in a particular characteristic frequency of the defect. A frequency match between the driving ultrasonic wave and this characteristic frequency provides a Local Defect Resonance (LDR) and results in efficient energy delivery from the wave into the defect. In this paper, such a selective ultrasonic activation of resonant defects is suggested to enhance nonlinear ultrasonic, optical and thermal defect responses. Multiple case studies demonstrate that the resonant excitation of a defect results in a high local vibration and enhancement of sensitivity in ultrasonic NDT and imaging of defects via laser vibrometry, thermosonics, nonlinearity and shearography readily measurable even for a few mW of ultrasonic power. The LDR-based NDT methods require much lower ultrasonic power to activate the defects that makes it possible to avoid high-power ultrasonic instrumentation.

Introduction

The interaction of elastic waves with defects is the background of ultrasonic imaging and nondestructive testing (NDT) of materials and industrial components. In conventional ultrasonic NDT, this interaction is responsible for sound attenuation and scattering (primary ultrasonic effects) which results in variation of the wave amplitude and phase as indicators of the presence of defects. The derivative ultrasound-induced effects (nonlinear, thermal, acousto-optic) are more advantageous in many cases and also widely used for NDT and defect imaging. However, these effects are usually comparatively inefficient so that the corresponding NDT techniques (nonlinear ultrasonics, ultrasonic shearography (shearosonics) and ultrasonic thermography (thermosonics)) require an elevated acoustic power and differ from conventional NDT set-ups for their specific instrumentation.

In our studies, it was proposed to enhance acoustic response of a defect by using selective acoustic activation of defects based on the concept of Local Defect Resonance (LDR) [1, 2]. In the general case, the presence of a defect apparently leads to a local decrease in stiffness for a certain mass of the material around the damaged area, which should manifest in a particular characteristic frequency (ω_0) of the defect. The frequency match between the driving wave and ω_0 results in the high-amplitude defect resonance vibrations and thus provides an efficient delivery of acoustic energy directly into the defect. The resonance acoustic response ensures a boost in efficiency and sensitivity of defect detection and imaging by using both primary and secondary ultrasonic effects.

1. LDR: Phenomenology and FEM Simulation

The LDR frequency can be introduced as a natural frequency of the defect with an effective rigidity K_{eff} and mass M_{eff}: $f_0 = \frac{1}{2\pi}\sqrt{K_{eff}/M_{eff}}$. To derive the expressions for K_{eff} and M_{eff} one should evaluate the potential and kinetic vibration energy of the defect. To clarify the physical nature of LDR this approach is applied to model defects such as flat-

bottomed holes (FBH). For a circular FBH (radius R, thickness h), the expressions obtained are:

$$K_{eff} = 192\pi D / R^2 ; M_{eff} = 1.8m , \quad (1)$$

while for a square FBH (side a and thickness h):

$$K_{eff} = 32\pi^4 D / a^2 ; M_{eff} = 2.25m , \quad (2)$$

where $D = Eh^3 / 12(1-\nu^2)$ is the bending stiffness, E is Young`s modulus, $\nu$ is Poisson`s ratio, and m are the masses of the plates with density ρ in the bottom of the defect.

Equations (1-2) are then combined to yield the LDR frequencies for the defects in question:

$$f_0 = \frac{10h}{3\pi R^2}\sqrt{\frac{E}{5\rho(1-\nu^2)}} . \quad (3)$$

$$f_0 = \frac{4\pi h}{3a^2}\sqrt{\frac{E}{6\rho(1-\nu^2)}} . \quad (4)$$

The expressions for f_0 are applicable to evaluation of the fundamental resonance frequencies of the defects, like FBH as well as laminar defects in rolled sheet metals and delaminations in composites. The problem in practical use of the analytical approach is concerned with the boundary conditions for the defect edges, which were assumed to be clamped in deriving (3) & (4). Instead, the finite element simulation was used to visualize the LDR vibration patterns and to evaluate the LDR frequencies.

The software COMSOL MULTIPHYSICS (physics package “structural dynamics,” “eigenfrequency analysis”) was found to be suitable for analyzing the vibration characteristics of structures with defects and to determine the LDR frequencies. Figure 1 illustrates the vibration pattern at frequency 8255 Hz, which is readily identified as a fundamental LDR of a square FBH ($h = 1.2$ mm; $a = 2$ cm). A similar “bell-like” vibration

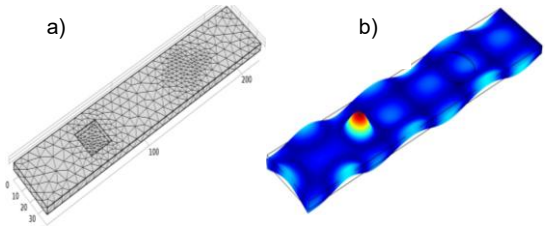

Fig. 1. FEM mesh (a) and fundamental LDR vibration pattern at $f_0 = 8255$ Hz (b) for 2x2 cm^2 square FBH in a PMMA plate.

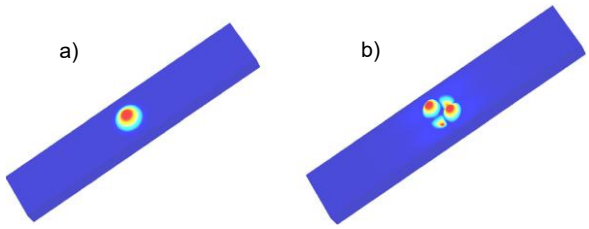

Fig. 2. A fundamental LDR (10.4 kHz) (a) and higher-order LDR (23.25 kHz) (b) for a FBH (radius 1 cm, depth 2 mm) in a PMMA plate.

pattern reveals a fundamental LDR in a circular FBH at frequency 10.4 kHz (Fig. 2 (a)), followed by the higher-order LDR at the higher driving frequency of 23.25 kHz (Fig. 2 (b)).

2. Resonant Defect Imaging

2.1 Resonant Laser Vibrometry

To experimentally identify the value of LDR frequency an ultrasonic excitation by a wide-band piezo-transducer is combined with a laser vibrometer (PSV 300 Polytec) scan of the specimen surface. It enables to probe and indicate all possible resonances in every point of the specimen. A strong enhancement of the vibration amplitude observed locally in the defect area is identified as a fundamental defect resonance and used for defect activation and imaging at this frequency.

Figure 3 illustrates LDR frequency responses and the vibration patterns measured for a simulated (circular FBH in PMMA plate) and a realistic defect (impact damage in carbon fiber reinforced composite (CFRP)).

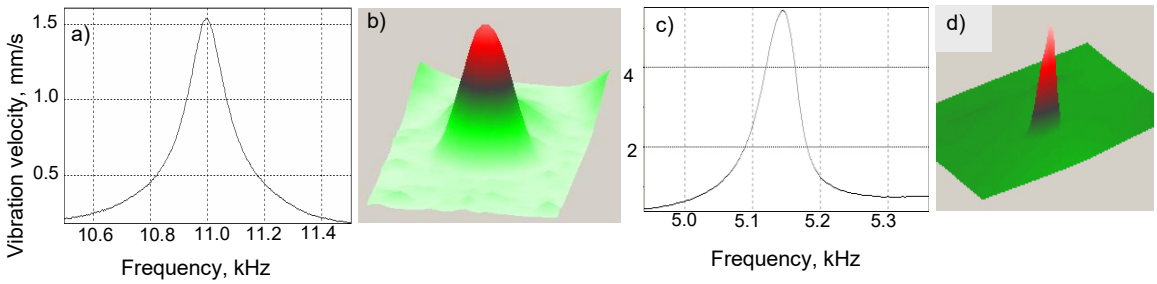

Fig. 3. LDR frequency responses and vibration patterns for a circular flat-bottomed hole (radius a=1 cm; depth h=0.8 mm) in PMMA plate (200x30x3mm^3) (a, b) and impact damage in CFRP plate (c, d).

LDR features a strong enhancement of the vibration amplitude confined strictly inside the defect areas with high Q-factors (in Fig. 3, $Q \approx 75$ for FBH and $Q \approx 85$ for the impact damage). The value of Q factor determines the resonance "amplification" of the vibration amplitude. Similar measurements showed that the quality factors in the range of 10-100 are typical for realistic defects in composites so that the LDR induced enhancement in sensitivity of defect imaging as high as ~ 20-40 dB was usually observed. Alternatively, the enhanced sensitivity enables to reduce the input acoustic power by orders of magnitude.

2.1 LDR Nonlinear NDT and Defect Imaging

Nonlinear acoustic NDT recognised as a promising technology for diagnostics of incipient damage is based on the frequency conversion (e.g. generation of higher harmonics, mixing frequencies) due to nonlinearity of defects caused by Contact Acoustic Nonlinearity (CAN). However, the low efficiency of conversion from fundamental frequency to nonlinear frequency components is the bottleneck problem of nonlinear ultrasonic applications in NDT. The use of LDR, which "amplifies" local defect vibrations, enables to enhance the sensitivity of the technique and reduce dramatically the acoustic power required to develop the nonlinearity.

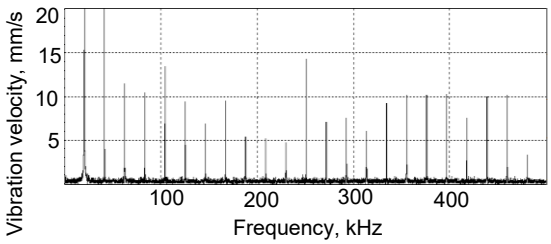

Fig. 4. HH spectrum for delamination in glass fiber reinforced (GFRP) specimen driven at LDR frequency 20900 Hz. Input voltage is 7V.

An extremely high resonant nonlinearity is demonstrated in Fig. 4 for a delamination in GFRP plate: Multiple higher harmonic (HH) generation is observed in the defect area while driving the specimen at LDR frequency even at moderate input voltage.

A high quality factor of LDR can also be used as an "amplifier" in the frequency mixing nonlinear NDT. This method is based on the nonlinear interaction of ultrasonic

waves of different frequencies (f_1, f_2) that results in a combination frequency output: $f_{\pm} = f_1 \pm f_2$.

According to the experiments [3], under resonance conditions nearly total input energy at fundamental frequency can be converted into HH or subharmonic vibrations of the defects. This suggests nonlinear LDR application as an extremely efficient mode in nonlinear NDE. In the experiments and applications, the input electric power is usually well below 1W; general purpose piezo-ceramic transducers (Conrad Elektronik GmbH) are used for ultrasonic excitation without any particular filtering of the input signals. Besides, due to LDR the nonlinear vibrations are being confined inside the defect area. This makes LDR nonlinearity inherently defect-selective and provides the background for defect-selective nonlinear imaging of fractured flaws.

The benefit of the higher harmonic LDR imaging is illustrated in Fig. 5. A substantial improvement of the image quality (10x20 mm^2 delamination in a GFRP plate) is clearly seen by comparing the fundamental (signal-to-noise ratio ~12 dB) and the second harmonic (signal-to-noise-ratio ~24 dB) images.

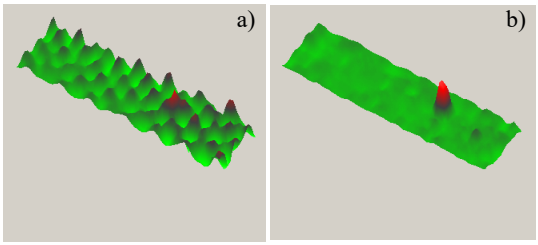

Fig. 5. Linear (36.77 kHz, a) and second harmonic (73.53 kHz, b) LDR imaging of a delamination in GFRP specimen.

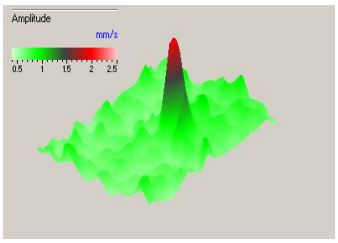

Fig. 6. Sum-frequency image of impact damage (~5x5mm^2) in a CFRP plate.

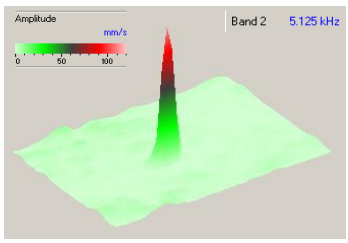

Fig. 7 Subharmonic LDR imaging of impact damage: Input 10250 Hz; output 5125 Hz.

Other examples of the resonance nonlinear imaging are given in Figs. 6, 7. The LDR contribution to the sum-frequency signal makes it localized in the damage area and enables to be used for mixing frequency imaging with reasonable signal-to-noise level (SNR) (~15 dB, Fig. 6). This image of the impact in a CFRP plate was obtained by mixing flexural waves of frequencies 77 kHz and 30 kHz via combination frequency resonance (LDR frequency of the defect 107 kHz). An example of subharmonic LDR imaging with an excellent SNR ≥ 35 dB is illustrated in Fig. 7 for the impact damage in CFRP specimen.

2.2 Resonant Thermosonics

To provide a measurable temperature response, thermosonics traditionally relies on high-power ultrasonic welding equipment, which includes kW-power supply (at fixed frequencies 20 or 40 kHz) and piezo-stack converters combined with ultrasonic boosters and horns. To make ultrasonic thermography compatible with conventional ultrasonic equipment would be a step on the way to extend its applicability in nondestructive inspection. To this end, an obvious task is to find out a feasibility of thermosonics in the mW-acoustic power range typical for commercial ultrasonic applications.

The LDR-induced amplification of local vibrations is, therefore, beneficial for enhancement of acousto-thermal conversion and would enable to reduce acoustic power required for thermosonic imaging. Figure 8 illustrates the benefit of LDR thermosonic imaging of the square insert in CFRP specimen. A crucial role of LDR is readily seen: At fundamental LDR frequency (8980 Hz) the temperature response (~0.25 K) is by more than an order of magnitude higher than that outside the LDR (8000 Hz).

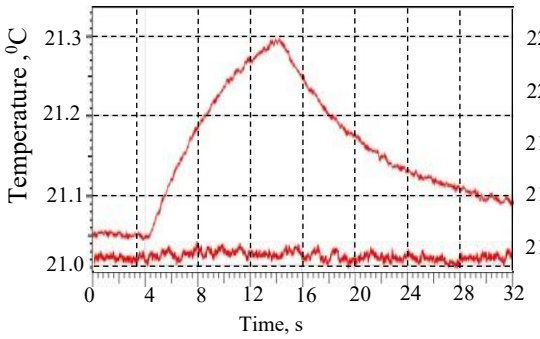

Fig. 8. Temperature response of a rectangular inset in CFRP plate at LDR frequency (8980 Hz, upper curve) and outside resonance (lower curve, 8000 Hz).

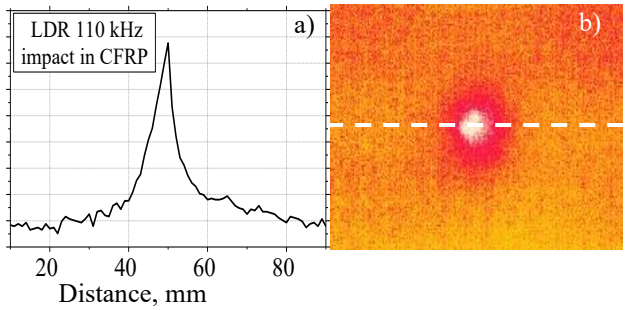

Fig. 9. LDR thermosonic imaging of ~(5x5 mm^2) impact damage area in a CFRP plate (b); quantified temperature contrast of the image along the dotted line (a).

To quantify the contribution of LDR to thermosonics output the temperature response of this defect is measured for calibrated ultrasonic power obtained with laser vibrometry. The data in Fig. 9, a) confirms highly efficient LDR thermosonics: ΔT = 1.4 K for ~60 mW input acoustic power. Such temperature variation provides reliable imaging in mW power range with a high temperature contrast in lateral direction (Fig. 9 b).

By introducing the benefit of LDR in the lock-in approach [4] a resonance thermosonic mode operating at unusually low excitation levels can be projected. The enhancement in sensitivity and the signal-to-noise-ratio of LDR lock-in imaging are readily seen from Fig. 10, where the amplitude lock-in (a) and LDR temperature (b) thermosonic images of a circular FBH in PMMA plate are shown. To have the SNR>1 directly in the temperature image (without lock-in) (Fig. 10 b), the input power had to be increased by up to ~2 mW (to generate $\Delta T \sim 100$ mK). On the contrary, the LDR lock-in image in Fig. 10 a) was taken when the input was reduced to anomalously low power of ~ 200 μW. The background for such an extraordinary performance is a combined action of the lock-in and the high thermosonic quality factor (efficient heat generation) in the LDR mode.

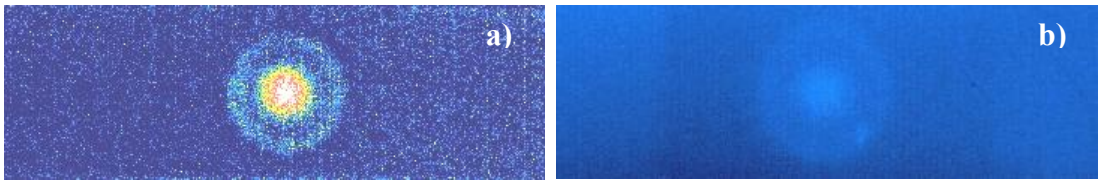

Fig. 10. LDR thermosonic imaging of FBH in PMMA plate at LDR frequency 7670 Hz: (a) - amplitude lock-in image (acoustic input ~200 μW); (b) – temperature image at input power ~ 2 mW.

Figure 11 illustrates the enhancement in sensitivity of thermosonics by combining LDR

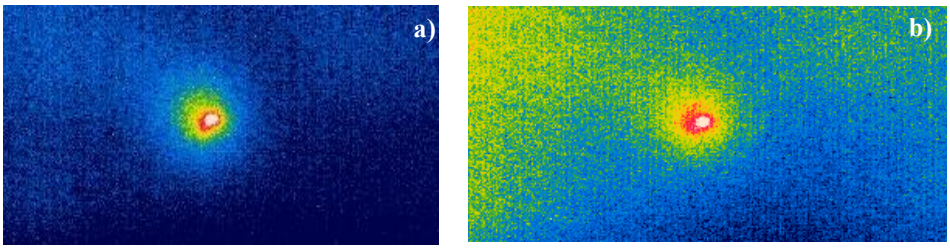

Fig. 11. LDR thermosonic imaging of an impact (~5x5 mm^2) in CFRP plate: amplitude lock-in image (a) at ~ 1mW input acoustic power; (b) – temperature image at ~16 mW input power.

and lock-in for an impact damage in a CFRP plate: the amplitude lock-in image (a) corresponds to ~1 mW input power while a similar contrast of the temperature image (b) requires ~16 mW of acoustic power.

2.3 LDR Shearosonics

In the experiment, the specimen is excited at LDR frequency in continuous ultrasonic generation mode by using piezo-transducers. An out-of-plane optical sensor head [5] with continuous-wave laser and CMOS digital camera (frame rate 200 Hz) was used for defect imaging. The speckle pattern of a vibration object is integrated over the frame period and compared with a reference (undeformed state) speckle.

In Fig. 12, the laser vibrometer and ultrasonic shearography images of a FBH vibration in PMMA specimen obtained at the fundamental LDR (7672 Hz) are compared. The 'butterfly' fringe pattern (Fig. 12, a)) clearly demonstrates that shearography is sensitive to the gradient of out-of-plane LDR displacement ("bell-like" function in Fig. 12, c) in the shearing (horizontal) direction. The increase in out-of-plane vibration amplitude due to LDR provides a strong increase in the corresponding strain and thus enhancement of sensitivity in LDR shearography mode.

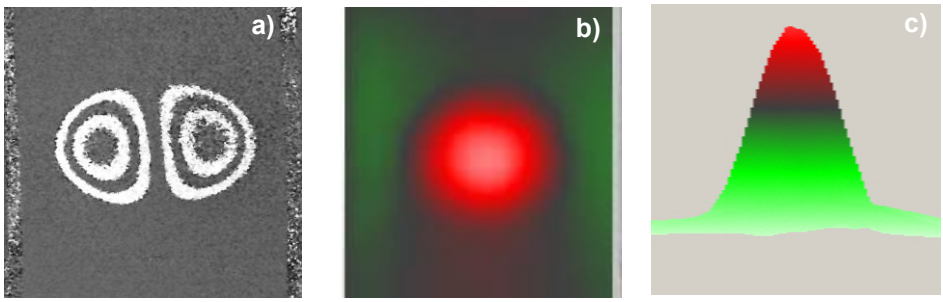

Fig. 12. Sherographic (a) and laser vibrometer images (b (top view), c (side view)) of a FBH vibration in PMMA plate at fundamental LDR (7672 Hz).

The effect of LDR shearography is demonstrated in Fig. 13 for aluminium honeycomb structure (thickness 16 mm) with several inclusions of resin and water in GFRP liners (0.5x100x100 mm^2). The laser vibrometry scan of the front side indicates fundamental LDR of one of the defects at 14940 Hz. The ultrasonic excitation for LDR shearography was carried out by conventional piezo-ceramic transducers (Conrad Elektronik GmbH) attached to the rear side of the structure. The results of both shearographic and thermosonic imaging (Fig. 13) confirm substantial enhancement of the sensitivity of detection at the

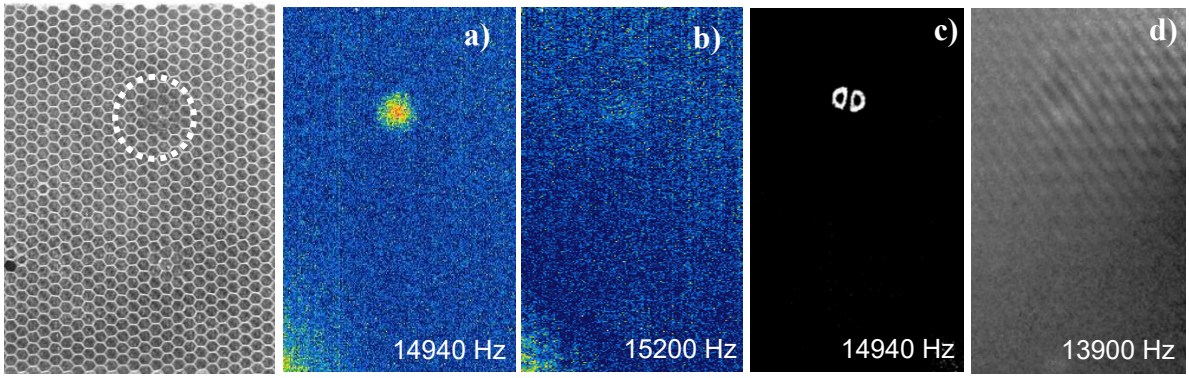

Fig. 13. Impact of frequency mismatch on LDR thermosonic (a, b) and shearographic (c, d) imaging of an adhesion lack area in honeycomb structure (left): the excitation frequencies are indicated on the images.

LDR frequency: the images practically disappear even at a minor frequency mismatch from the LDR frequency (Fig. 13).

To trace frequency selectivity of LDR shearographic imaging we used a set of three circular FBH in a PMMA plate. For the plate thickness of 25.5 mm, the depths of the holes changed from 22 to 24 mm thus defining different LDR frequencies and driving excitation frequencies, respectively. The images of the defects obtained by the laser vibrometry, thermosonics and shearography at corresponding LDR frequencies are compared in Fig. 14. They confirm maximum sensitivity at the LDR frequencies; a minor variation of the frequencies is caused by different clamping conditions of the specimens.

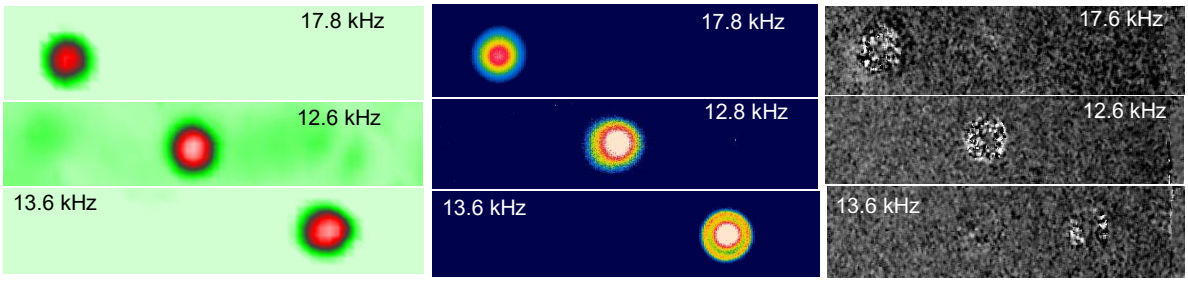

Fig. 14. LDR laser vibrometer (top), thermosonic (center) and shearographic (bottom) images of three circular FBH in PMMA specimen: the frequencies of maximum output are indicated on the images.

3. Conclusions

In summary, the frequency match between the excitation ultrasonic frequency and the frequency of LDR results in substantial "amplification" of the defect vibration amplitude. It leads to enhancement of sensitivity and efficiency in ultrasonic NDT and imaging of defects via nonlinearity, laser vibrometry, thermosonics and shearography. A strong frequency selectivity of LDR results in opportunity of detecting a certain defect among a multitude of others by using all above mentioned NDT methods. The LDR NDT requires much lower acoustic power to activate the defects that makes it possible to avoid high-power instrumentation and use conventional ultrasonic equipment instead.

References

[1]. Solodov, I., Bai, J., Bekgulyan, S., Busse, G. A local defect resonance to enhance acoustic wave-defect interaction in ultrasonic nondestructive testing, *Applied Physics Letters* 99, 211911 (2011).

[2]. Solodov, I., Bai, J., Busse, G. Resonant ultrasonic spectroscopy of defects: Case study of flat-bottomed holes, *Journal of Applied Physics* 113, 223512 (2013).

[3]. Solodov, I. Resonant acoustic nonlinearity of defects for highly-efficient nonlinear NDE, *Journal of Nondestructive Evaluation*, 33, 252-262 (2014).

[4]. Busse, G., Wu, D., Karpen, W. Thermal wave imaging with phase sensitive modulated themography, *Journal of Applied Physics* 71 (8), 3962-3965 (1992).

[5]. Menner, P., Gerhard, H., Busse, G. Remote defect visualization with thermal phase angle shearography, *AIP Conference Proceedings* 1211 (1), 2068-2072 (2010).